Late Ediacaran paleogeography of Avalonia and the Cambrian assembly of West Gondwana

Bin Wen[1, 2,*], David A.D. Evans[1], Ross P. Anderson[3, 4], Phil J.A. McCausland[5]

[1]Department of Earth and Planetary Sciences, Yale University, 210 Whitney Avenue, New Haven, CT, 06511

[2]State Key Laboratory of Geological Processes and Mineral Resources, School of Earth Sciences, China University of Geosciences, Wuhan 430074, China

[3]All Souls College, University of Oxford, Oxford, OX1 4AL, UK

[4]Department of Earth Sciences, University of Oxford, Oxford OX1 3AN, UK

[5]Western Paleomagnetic and Petrophysical Laboratory, Department of Earth Sciences, University of Western Ontario, 1151 Richmond Street, London, Ontario, N6A 5B7, Canada

*E-mail: benwen2013@gmail.com; wenbin@cug.edu.cn. Current address at: State Key Laboratory of Geological Processes and Mineral Resources, School of Earth Sciences, China University of Geosciences, Wuhan 430074, China

Abstract

The latest Proterozoic tectonic evolution of Avalonia, one of the largest peri-Gondwanan terranes, bears on the issue of Gondwana amalgamation during the transition from Rodinia to Pangea. New paleomagnetic results from mid–late Ediacaran strata in the Newfoundland sector of Avalonia confirm substantial apparent motion of that terrane between ca. 590 and 560 Ma, consistent with a true polar wander interpretation for that interval. When the Avalonian poles are mapped onto complementary paleomagnetic records from West Africa and Laurentia, the Avalonia terrane may occupy any of four possible positions, all of which are far-removed from those cratons. Choosing the most kinematically parsimonious location leading toward Gondwana assembly, we find that Avalonia was most likely proximal to Amazonia during the Ediacaran–Cambrian transition, with a substantial (~3000 km) separation between Amazonia and West Africa at that time. Our results thus favor the existence of a wide Clymene Ocean and subsequent Cambrian final assembly of West Gondwana**,** providing a key snapshot onto the evolving Rodinia-Gondwana supercontinental transition.

Keywords

Avalonia terrane, Paleomagnetism, True polar wander, Clymene Ocean, West Gondwana

1. Introduction

The timing of orogenic assembly among Gondwana cratons is crucial to testing the existence of hypothetical supercontinent Pannotia (Murphy and Nance, 1991) and thus evaluating the supercontinental cycle in general terms. Within West Gondwana, the most contentious debate on cratonic assembly concerns the timing of Amazonia's accretion to its Gondwana neighbors. Some researchers advocate that West Gondwana had welded together before ca. 600 Ma (e.g., Cordani et al., 2013); whilst others suggest that a substantial seaway (Clymene Ocean) between Amazonia and other Gondwana cratons was not completely closed until Cambrian time (e.g., Trindade et al., 2006; Tohver et al., 2010, 2012; McGee et al., 2015; Schmitt et al., 2018). Although recent key paleomagnetic poles from West Africa (Robert et al., 2017) show dramatic polar motions during mid–late Ediacaran time, the lack of definitive Ediacaran paleomagnetic poles from Amazonia leave the controversy unresolved (D'Agrella-Filho et al., 2016).

Kinematic constraints from peri-Gondwanan terranes may assist in resolving this kind of controversy, if their motions can be linked plausibly to once-adjacent, larger cratons (i.e., to Amazonia). Avalonia is one of the largest peri-Gondwanan terranes, and its geological record provides important constrains on the tectonic history of the supercontinental transition from Rodinia to Pangea (e.g., Murphy et al., 2000, 2004, 2019; Pollock et al., 2012). Most current Rodinia reconstructions show Avalonia proximal to a nexus of West Africa, Amazonia, and Baltica (e.g., Pisarevsky et al., 2008; Li et al., 2013; Cawood et al., 2016). After Rodinia breakup (<750 Ma), different portions of Avalonia show distinct

stratigraphic and geochronologic-isotopic affinities to these cratons, namely East Avalonia to West Africa (e.g., Nance and Murphy, 1994; Waldron et al., 2019), and West Avalonia to either Amazonia or Baltica (e.g., Pollock et al., 2009; Thompson et al., 2012; Henderson et al., 2016; Murphy et al., 2019). Herein, we present new Ediacaran paleomagnetic results from Avalonia in its type locality of Newfoundland, Canada (Fig. 1), and establish a definitive apparent polar wander path (APWP) segment for that terrane. Integrating the new data with compiled poles from neighboring cratons, we favor an Avalonia-Amazonia juxtaposition that is separated from proto-Gondwana, providing a new interpretation for the Ediacaran–Cambrian paleogeography and assembly of West Gondwana.

2. Geological settings

Avalonia is one of the largest peri-Gondwanan terranes within the Appalachian-Caledonide-Variscan belt, and is subdivided into West Avalonia (in New England and Nova Scotia-Newfoundland, North America) and East Avalonia (in Europe) (Fig. 1A; Henderson et al., 2016; Murphy et al., 2019). Across the entire Avalonia terrane, there is no crystalline basement exposed. Precambrian–early Paleozoic strata from both subunits include early (ca.760–660 Ma) and main (ca.635 Ma) stage arc-related rocks, and late stage (<590 Ma) rift-related volcanic and sedimentary successions (Murphy et al., 2008; Henderson et al., 2016). The latter part of the successions hosts Ediacaran Biota and Cambrian–Ordovician Acado-Baltic faunas (O'Brien et al.,1996; Pollock et al., 2009).

The ‘Avalon Zone’ in southeastern Newfoundland represents the core portion of West Avalonia, and is bounded to the northwest by Ganderia along the Dover-Hermitage Bay Faults (Fig. 1B; O'Brien et al.,1996). Our study area lies in the northwest (Bonavista Peninsula) of the ‘Avalonia Zone’ (Fig. 1B) and was deposited within the Bonavista Basin according to regional mapping (Normore, 2011). The strata include volcanic arc and deep marine successions of the Love Cove and Connecting Point groups (Mills et al., 2016), and subaerial volcanic and shallow-marine to terrestrial deposits of the overlying Musgravetown Group (Normore, 2010, 2011). In the sampling area, the Musgravetown Group unconformably overlies the >605 Ma Connecting Point Group (Mills et al., 2016) and its top is truncated by the early Cambrian quartzitic Random Formation (O'Brien et al.,1996; Normore, 2010). The total thickness of this group exceeds 4000 m and contains the Bull Arm Formation predominantly bimodal volcanic rocks, Big Head Formation siltstone, Rocky Harbour Formation sandstone, and Crown Hill Formation sandstone/siltstone interbedded with massive conglomerate (Normore, 2010, 2011; Pu et al., 2016). Within the Rocky Harbour Formation, the (ca. 580–579 Ma) Gaskiers glacial diamictites are well preserved (Pu et al., 2016). Together with the updated geochronologic (U-Pb) data (Pollock et al., 2009; Mills et al., 2016, 2017; Pu et al., 2016), the ages for the Musgravetown Group successions are well constrained (Fig. 1C). At its base, the eruption age for the Bull Arm Formation volcanic rocks is constrained to ca. 592 Ma by U-Pb zircon ages from two tuff beds (592 ± 2.2 Ma and 591.3 ± 1.6 Ma; Mills et al., 2017). While at its top, the Crown Hill Formation unconformably overlies the Rocky Harbour Gaskiers-age

glacial deposits and is unconformably overlain by the earliest Cambrian Random Formation (Fig. 1C; Pollock et al., 2009; Normore, 2010, 2011; Pu et al., 2016). Considering further the two youngest detrital zircon ages (557 ± 14 Ma and 566 ± 13 Ma) from the most upper portion of this formation (Fig. 1C; Pollock et al., 2009), the age of the Crown Hill Formation is approximately constrained to 560 Ma. Gentle folding during Silurian–Devonian docking of Avalonia to Laurentia (Normore, 2010, 2011) provides opportunity for a paleomagnetic field stability test on the studied rocks.

3. Methods

Samples were collected along five geologic sections at three localities: Tickle Cove-Duntara, Clifton, and Hodge's Cove-Nine Angle Pond (Figs. 1B and 2), encompassing the Bull Arm, Big Head, Rocky Harbour and Crown Hill formations. Most were drilled as oriented cores in the field, and a small number were block-sampled. Magnetic compasses provided sample azimuthal orientation and solar compasses were used whenever possible for the correction of local magnetic declination. Remanent magnetizations were measured using a 2G-Enterprises DC-SQuID magnetometer, which is equipped with an automatic sample-changing system (Kirschvink et al., 2008) in a magnetically shielded laboratory at Yale University. After measuring the natural remanent magnetization (NRM), all samples were thermally demagnetized with an average of ≥16 incremental steps (Fig. 3), until heating to 600 °C (for basalts) and 690 °C (for sandstones/siltstones) or thoroughly demagnetized/unstable. For the basalts, an additional

126 liquid-nitrogen cooling step was made before heating to remove viscous magnetizations of
127 multidomain magnetite (Dunlop and Argyle, 1991). Magnetic remanence directions were
128 defined using principal-component analysis (Kirschvink, 1980). The software packages
129 Paleomag (Jones, 2002) and PaleoMac (Cogné, 2003) were used for data analysis and
130 figure production.
131
132 **4. Results**
133 Overall, remanence directions from the rocks of the upper portion (Crown Hill Formation)
134 of the Musgravetown Group are more stable and consistent than those from the lower
135 portion. Directions from the Bull Arm and Big Head formations are highly scattered
136 (within site/same formation) or unusable (Table 1; Fig. 3A-C). Only two sites from the
137 Bull Arm Formation yielded the characteristic SW-down and NE-up directions (Fig. 3A
138 and B) as measured previously from the Bonavista Basin (Fig. 1B) by Pisarevsky et al.
139 (2012). Put together, the maximum concentration of the characteristic remanent
140 magnetizations (ChRMs) occurs in the range 41–137% unfolding at the 95% confidence
141 level (Fig. 4C; Tauxe et al., 2016). The result for this test is probably biased by the low
142 number of sites applied, but three positive conglomerate tests and a baked contact test
143 (Pisarevsky et al., 2012) in this region strongly support a primary origin for the remanence.
144 Thus, a combined paleomagnetic pole ('BA-b'; Tables 1 and 2) for the ca. 592 Ma Bull
145 Arm Formation at Bonavista is calculated at λ=-15.5°N, φ=278.2°E, A_{95}=11.9° with a
146 paleolatitude of 21.3 ± 9.1°. An indistinguishable pole relying on the dataset of Pisarevsky

147 et al. (2012) is also calculated (λ=-14.0°N, φ=277.9°E, A_{95}=14.2°) for comparison. For the
148 Rocky Harbour Formation, ChRMs are inconsistent between different sites (Table 1). An
149 inconclusive conglomerate test (Fig. 5) suggests that their reliabilities are questionable and
150 are excluded from further discussion.
151
152 In contrast, samples from the overlying Crown Hill Formation shared broadly similar
153 characteristics to each other, exhibiting one single (Fig. 3E) or two magnetic components
154 (Fig. 3F): low-(below 300–500°C; LTC) and high-temperature (up to 650–690°C hematite
155 range; HTC) components. The LTC directions are parallel to the present Earth's field (PEF;
156 Fig. 6A) and become scattered after tilt correction (Fig. 6B), representing a viscous
157 magnetization of recent field. Both the HTCs and single stable components linearly decay
158 to the origin (Fig. 3E and F) or rarely along a demagnetization plane through the origin,
159 defining the ChRMs which show dipolar-intermediate NW-down/SW-up directions (Fig.
160 4A and B). The ChRMs pass a parametric bootstrap fold test (Fig. 4D; Tauxe et al., 2016)
161 and a reversal test at the 95% confidence level (class 'B'; McFadden and McElhinny,
162 1990). An average site-mean direction for the combined polarities is calculated at D_g =
163 133.6°, I_g = -55.7°, k_g = 14.4, α_{95}= 5.4°; D_s = 140.2°, I_s = -37.7°, k_s = 31.1, α_{95}= 3.6° (n = 51
164 sites), yielding a new paleopole ('CH') at λ=-48.1°N, φ=09.9°E, A_{95}=3.3°.
165
166 **5. Discussion**
167 *5.1. Apparent polar wander path of Avalonia and its implications*

Our results largely reproduce those presented by Pisarevsky et al. (2012) from the same formations, but we augment their dataset with Crown Hill Formation sites that lie within the typical northeasterly tectonic grain of the Bonavista Peninsula (Fig. 1B). Thus, we are able to show that the Bull Arm versus Crown Hill remanences' azimuthal directional discordance is not due to local rotations; the Newfoundland sector of West Avalonia can be considered as a quasi-rigid block for the purposes of terrane reconstructions. Integrating our new results with the compiled paleopoles (with Q-factor >3; Van der Voo, 1990) from West Avalonia of Newfoundland (Table 2), a segment of APWP for this terrane is defined, showing a large (~90°) polar motion from ca. 590–575 to 560 Ma (Fig. 7A). A reconstructed Avalonia composite terrane is also resolved by fitting the Ediacaran poles from New England, Newfoundland, and England (Fig. 7A; Table 2).

The substantial arc distance between mid- and late-Ediacaran poles (~90° over a timespan of merely ~20–30 Myr) from Avalonia is reminiscent of the comparable distances within APWPs of both Laurentia (McCausland et al., 2011; Mitchell et al., 2011) and West Africa (Robert et al., 2017, 2018) over the same time interval. To explain these kinds of variant datasets, Abrajevitch and Van der Voo (2010) proposed an equatorial geomagnetic dipole hypothesis, whereas Robert et al. (2017, 2018) interpreted them as recording inertial interchange true polar wander (IITPW). Although the contribution of an equatorial dipole field during the polarity reversals is permissible (Halls et al., 2015), the available data overall weighs more towards the IITPW process. As pointed out by many researchers (e.g.,

McCausland et al., 2007, 2011; Bono and Tarduno, 2015; Robert et al., 2017, 2018), the multiple-component (steep and shallow) directions from a same rock unit are not equally reliable (reviewed in Robert et al., 2017). Adopting that methodology of data selection based purely on reliability rather than *a priori* judgment of tectonic implications, the most robust poles from Laurentia and West Africa (Table S1; Robert et al., 2017, 2018) define a similar trend of APWPs from ca. 590–575 to 560 Ma (Fig. 7B) and a polar-motion rate is calculated at ~2–9°/Ma (including this study). This rate is consistent with a plausible speed of TPW (e.g., Steinberger and Torsvik, 2008; Greff-Lefftz and Besse, 2014; Robert et al., 2018). Additionally, the quasi-static Sutton hotspot under Laurentia suggests stability of that plate relative to a deep mantle reference frame, which can be adequately explained by TPW in this interval (Mitchell et al., 2011).

After rotating Avalonia around an Euler pole (5.8°S, 158.8°E, -84.1°) to fit its two groups (~590–575 and 560 Ma) of poles with those of West Africa and Laurentia (Table S1; Robert et al., 2017, 2018), a composite alignment of APWPs for the continents of West Gondwana is achieved, and a large distance between Avalonia and West Africa is implied (Fig. 7B). The effects of possible inclination shallowing (using a nominal value of f=0.6; dashed 'CH' ellipse in Fig. 7B) are minor at this scale of APWP. Due to ambiguous geomagnetic polarity and ~90° separation between the poles of Avalonia, we consider four possible relative positions of Avalonia and West Africa (positions 1-4; Fig. 7B), none of which allow a direct Avalonia-West Africa juxtaposition. Among the four possibilities,

position #1 seems the most reasonable because: (i) it readily accommodates a transition toward West African sources of detritus for early Cambrian Avalonian sediments (Waldron et al., 2019), and (ii) it provides the most feasible way for Avalonia to drift from southern-hemisphere Gondwana (e.g., Torsvik et al., 2012) to eventual accretion with Laurussia in a right-way-up orientation at moderate southerly latitudes during the mid-Paleozoic time (Murphy et al., 2019).

5.2. Paleogeography of West Gondwana

It is well documented that Avalonia had accreted to a larger cratonic margin by ca.650–630 Ma (e.g., Murphy et al., 2000, 2019), as evidenced by localized high-grade metamorphism in some parts of Avalonia (e.g., O'Brien et al.,1996; Murphy et al., 2004) and an isotopic shift to more evolved crustal sources (Henderson et al., 2016). One of the previously suggested options for that connection is a location ('X' in Fig. 8A) near West Africa, Amazonia, and the southern margin of Baltica (Thompson et al., 2012). By this conventional interpretation, aligning the mid–late Ediacaran APWP segments of Baltica and West Africa (Fig. 8A) creates a gap that represents the most suitable position for Amazonia (Amazonia itself lacks reliable late Ediacaran paleomagnetic data; Fig. 8B). This model would resemble the pre-600 Ma assembly scenario for West Gondwana (e.g., Cordani et al., 2013); however, the location ('X') of Avalonia in this model is not permitted by our Crown Hill data at ~560 Ma, which instead would favor a late Ediacaran location on the Timanian side of Baltica (Fig. 8A and B). But in order for Avalonia to achieve its Early

Cambrian position near ‘X’ that is indicated by biogeography (e.g. Cocks and Fortey, 2009; Álvaro et al., 2013) and sedimentary provenance (Pollock et al., 2009; Henderson et al., 2016; Waldron et al., 2019), Avalonia would need to migrate around Baltica in a complicated terminal Ediacaran kinematic scenario, prior to Paleozoic separation and crossing of the Iapetus realm (e.g., Murphy et al., 2004, 2019; Pollock et al., 2009, 2012).

As an alternative model, we place Amazonia as the host craton adjacent to Avalonia—satisfying both basement isotopic similarities (Nance and Murphy, 1994) and sedimentary provenance (Pollock et al., 2009; Henderson et al., 2016). Baltica’s position, due to the uncertainty on the ages of the B-Kg and B-Bk (Kurgashlya and Bakeevo formations) paleopoles (Table S1; Robert et al., 2017), is adjusted to retain a loose connection with Avalonia (Thompson et al., 2012) and a broad APWP match with that of other cratons (Fig. 8C). The common potential source of 1.6–1.0 Ga zircons from both Baltica and Amazonia (Pollock et al., 2009; Henderson et al., 2016; Murphy et al., 2019) and a long-lived Meso- to early-Neoproterozoic connection with Laurentia (e.g., Pisarevsky et al., 2008) may provide some support for this juxtaposition. The ~635–570 Ma large strike-slip movements along Avalonia’s northern margin (current coordinates) (Murphy et al., 2004; van Staal et al., 2020) may have been caused by the separation of Baltica after its initial rifting from Laurentia at ca. 615 Ma during the opening of Iapetus Ocean (e.g., Pisarevsky et al., 2008). In this context, Amazonia becomes the only feasible host craton to Avalonia and the resulting configuration of West Gondwana at ca. 590–575

Ma in an absolute (TPW-based) reference frame is reached (Fig. 8D). In this model, subduction along the outboard active margin of Avalonia likely resulted in the development of the ca. 560–550 Ma blueschists in Anglesey-Lleyn of Wales, UK (Kawai et al., 2007). Moreover, this new model implies a ~3000 km wide Clymene Ocean between Avalonia-Amazonia and West Africa, compatible with the Ediacaran–Cambrian lithostratigraphic disparities between Avalonia and West Africa (e.g., Landing, 1996, 2005; Landing et al., 2013). Subsequently, West Gondwana was completely assembled by Cambrian time (Trindade et al., 2006; Tohver et al., 2010, 2012), and Avalonia migrated with Amazonia to arrive in proximity to West Africa as a result of that accretion. This amalgamation is consistent with the early Cambrian faunal similarities (such as trilobite genera) between Avalonia and the Western Mediterranean (e.g., Cocks and Fortey, 2009; Álvaro et al., 2013), and the collision could be represented by the early Cambrian Araguaia-Paraguai-Pampean belt (e.g., Tohver et al., 2010; Schmitt et al., 2018) related to Clymene Ocean closure (Fig. 8D). It is worth noting that, before that convergence, the Parnaíba (PR) and Río de La Plata (RP) blocks had been welded together with Central Gondwana by ca. 620–580 Ma (Fig. 8D; reviewed in Schmitt et al., 2018), corresponding to the earlier closure of the Goiás-Pharusian Ocean (or Pan-African-Brasiliano Orogens; Cordani et al., 2013; Ganade de Araújo et al., 2014; Schmitt et al., 2018). This scenario suggests that these paleocontinents witnessed both the early- and late-stage collisions within West Gondwana. Within that tectonic context, our data and model for mid–late Ediacaran time provide a key snapshot onto the evolving Rodinia-Gondwana

supercontinental transition, after final Rodinia breakup (Laurentia separating from Baltica and Amazonia) and prior to Gondwana amalgamation. A wide Clymene Ocean persisting after Iapetus opening negates the existence of the Pannotia supercontinent according to classic paleogeographic idealizations of that landmass (e.g., Dalziel, 1997).

Acknowledgements

This research was funded by a research grant to D. Evans from Yale University and by an ExxonMobil/Geological Society of America Student Geoscience Grant to R.P. Anderson. B. Wen is funded by the startup Grant (101-162301202620) from China University of Geosciences (Wuhan). R.P. Anderson acknowledges support from All Souls College and NASA (NNX14AP10H), as well as D.E.G. Briggs for helpful discussion. P.J.A. McCausland (NSERC – Discovery Grant) gratefully acknowledges funding support for this research. We appreciate insightful reviews from R. Schmitt, S. Pisarevsky, B. Murphy, and an anonymous reviewer on this and previous versions of the manuscript. We are also grateful to Editor An Yin for handling this paper. Great thanks are expressed to A. Mills (Newfoundland and Labrador Geological Survey) for helpful advice on field logistics and current perspectives on local Avalon field relationships, and to J. Hodych (Memorial University) for helpful discussion on previous paleomagnetic investigations and field assistance.

References

Abrajevitch, A., Van der Voo, R., 2010. Incompatible Ediacaran paleomagnetic directions suggest an equatorial geomagnetic dipole hypothesis. Earth Planet. Sci. Lett. 293, 164-170.

Álvaro, J. J., Ahlberg, P., Babcock, L. E., Bordonaro, O. L., Choi, D. K., Cooper, R. A., Ergaliev, G.K.H., Gapp, I.W., Pour, M.G., Hughes, N.C., Jago, J. B., Korovnikov, I., Laurie, J.R., Lieberman, B.S., Paterson, J.R., Pegel, T.V., Popov, L.E., Rushton, A.W.A., Sukhov, S.S., Tortello, M.F., Zhou, Z.Y., Zylinska, A., 2013. Global Cambrian trilobite palaeobiogeography assessed using parsimony analysis of endemicity. Geological Society, London, Memoirs 38, 273-296.

Bono, R.K., Tarduno, J.A., 2015. A stable Ediacaran Earth recorded by single silicate crystals of the ca. 565 Ma Sept-Oles intrusion. Geology 43, 131–134.

Cawood, P.A., Strachan, R.A., Pisarevsky, S.A., Gladkochub, D.P., Murphy, J.B., 2016. Linking collisional and accretionary orogens during Rodinia assembly and breakup: Implications for models of supercontinent cycles. Earth Planet. Sci. Lett. 449, 118-126.

Cocks, L. R. M., Fortey, R. A., 2009. Avalonia: a long-lived terrane in the Lower Palaeozoic?. Geol. Soc. Spec. Publ. 325, 141-155.

Cogné, J.P., 2003. PaleoMac: a Macintosh application for treating paleomagnetic dataand making plate reconstructions. Geochem. Geophy. Geosy. 4, 1–8.

Cordani, U. G., Pimentel, M. M., De Araújo, C. E. G., Basei, M. A. S., Fuck, R. A., Girardi, V. A. V., 2013. Was there an Ediacaran Clymene ocean in central South America? Am. J. Sci. 313, 517-539.

D'Agrella-Filho, M. S., Bispo-Santos, F., Trindade, R. I. F., Antonio, P. Y. J., 2016. Paleomagnetism of the Amazonian Craton and its role in paleocontinents. Braz. J. Geol. 46, 275-299.

Dalziel, I. W. D., 1997. OVERVIEW: Neoproterozoic-Paleozoic geography and tectonics: Review, hypothesis, environmental speculation. Geol. Soc. Am. Bull. 109, 16-42.

Dunlop, D.J., Argyle, K.S., 1991. Separating multidomain and single-domainlike remanences in pseudo-single-domain magnetites (215-540 nm) by low-temperature demagnetization. J. Geophys. Res. 96, 2007–2017.

Escayola, M. P., van Staal, C. R., Davis, W. J., 2011. The age and tectonic setting of the Puncoviscana Formation in northwestern Argentina: An accretionary complex related to Early Cambrian closure of the Puncoviscana Ocean and accretion of the Arequipa-Antofalla block. J. South Am. Earth Sci. 32, 438-459.

Ganade de Araújo, C.E., Rubatto, D., Hermann, J., Cordani, U.G., Caby, R., Basei, A.S., 2014. Ediacaran 2,500-km-long synchronous deep continental subduction in the West Gondwana Orogen. Nat. Commun. 5, 1-8.

Greff-Lefftz, M., Besse, J., 2014. Sensitivity experiments on True Polar Wander. Geochem. Geophy. Geosy. 15, 4599-4616.

Halls, H. C., Lovette, A., Hamilton, M., Söderlund, U., 2015. A paleomagnetic and U–Pb geochronology study of the western end of the Grenville dyke swarm: Rapid changes in paleomagnetic field direction at ca. 585 Ma related to polarity reversals? Precambrian Res. 257, 137-166.

Henderson, B. J., Collins, W. J., Murphy, J. B., Gutierrez-Alonso, G., Hand, M., 2016. Gondwanan basement terranes of the Variscan–Appalachian orogen: Baltican, Saharan

and West African hafnium isotopic fingerprints in Avalonia, Iberia and the Armorican Terranes. Tectonophysics 681, 278-304.
Jones, C.H., 2002. User-driven integrated software lives: “Paleomag”paleomagnetics analysis on the Macintosh. Comput. Geosci. 28, 1145–1151.
Kawai, T., Windley, B. F., Terabayashi, M., Yamamoto, H., Maruyama, S., Omori, S., Shibuya, T., Sawaki, Y., Isozaki, Y., 2007. Geotectonic framework of the Blueschist Unit on Anglesey–Lleyn, UK, and its role in the development of a Neoproterozoic accretionary orogen. Precambrian Res. 153, 11-28.
Kirschvink, J.L., 1980. The least squares line and the analysis of paleomagnetic data. Geophys. J. R. Astron. Soc. 62, 699–718.
Kirschvink, J.L., Kopp, R.E., Raub, T.D., Baumgartner, C.T., Holt, J.W., 2008. Rapid, precise, and high-sensitivity acquisition of paleomagnetic and rock-magnetic data: Development of a low-noise automatic sample changing system for su-perconducting rock magnetometers. Geochem. Geophys. Geosyst. 9, Q05Y01.
Landing, E., 1996. Avalon: Insular continent by the latest Precambrian, in Nance, R. D., and Thompson, M. D., eds., Avalonian and Related Peri-Gondwanan Terranes of the Circum–North Atlantic: Boulder, Colorado. Geological Society of America Special Paper 304, 27-64.
Landing, E., 2005. Early Paleozoic Avalon–Gondwana unity: an obituary—response to “Palaeontological evidence bearing on global Ordovician–Silurian continental reconstructions” by RA Fortey and LRM Cocks. Earth Sci. Rev. 1, 169-175.
Landing, E. D., Westrop, S. R., Bowring, S. A., 2013. Reconstructing the Avalonia palaeocontinent in the Cambrian: A 519 Ma caliche in South Wales and transcontinental middle Terreneuvian sandstones. Geol. Mag. 150, 1022-1046.
Li, Z. X., Evans, D. A., Halverson, G. P., 2013. Neoproterozoic glaciations in a revised global palaeogeography from the breakup of Rodinia to the assembly of Gondwanaland. Sediment. Geol. 294, 219-232.
McCausland, P. J., Hankard, F., Van der Voo, R., Hall, C. M., 2011. Ediacaran paleogeography of Laurentia: Paleomagnetism and 40Ar–39Ar geochronology of the 583 Ma Baie des Moutons syenite, Quebec. Precambrian Res. 187, 58-78.
McCausland, P. J., Van der Voo, R., Hall, C. M., 2007. Circum-Iapetus paleogeography of the Precambrian–Cambrian transition with a new paleomagnetic constraint from Laurentia. Precambrian Res. 156, 125-152.
McFadden, P. L., McElhinny, M. W., 1990. Classification of the reversal test in palaeomagnetism. Geophys. J. Int. 103, 725-729.
McGee, B., Collins, A. S., Trindade, R. I., Jourdan, F., 2015. Investigating mid-Ediacaran glaciation and final Gondwana amalgamation using coupled sedimentology and 40Ar/39Ar detrital muscovite provenance from the Paraguay Belt, Brazil. Sedimentology 62, 130-154.
McNamara, A. K., Niocaill, C. M., van der Pluijm, B. A., Van der Voo, R., 2001. West African proximity of the Avalon terrane in the latest Precambrian. Geol. Soc. Am. Bull. 113, 1161-1170.
Mills, A. J., Dunning, G. R., Murphy, M., Langille, A., 2017. New Geochronological constraints on the timing of magmatism for the Bull Arm Formation, Musgravetown Group, Avalon terrane, northeastern Newfoundland, in Current Research:

Newfoundland and Labrador Department of Natural Resources: Geological Survey Report 17-1, p.1-17.
Mills, A., Dunning, G., Langille, A., 2016. New geochronological constraints on the Connecting Point Group, Bonavista Peninsula, Avalon Zone, Newfoundland, in Current Research: Newfoundland and Labrador Department of Natural Resources: Geological Survey Report 16-1, p. 153-171.
Mitchell, R. N., Kilian, T. M., Raub, T. D., Evans, D. A., Bleeker, W., Maloof, A. C., 2011. Sutton hotspot: Resolving Ediacaran-Cambrian tectonics and true polar wander for Laurentia. Am. J. Sci. 311, 651-663.
Murphy, J. B., McCausland, P. J., O'Brien, S. J., Pisarevsky, S., Hamilton, M. A., 2008. Age, geochemistry and Sm–Nd isotopic signature of the 0.76 Ga Burin Group: Compositional equivalent of Avalonian basement?. Precambrian Res. 165, 37-48.
Murphy, J. B., Nance, R. D., 1991. Supercontinent model for the contrasting character of Late Proterozoic orogenic belts. Geology 19, 469-472.
Murphy, J. B., Nance, R. D., Keppie, J. D., Dostal, J., 2019. Role of Avalonia in the development of tectonic paradigms. Geol. Soc. Spec. Publ. 470, 265-287.
Murphy, J. B., Pisarevsky, S. A., Nance, R. D., Keppie, J. D., 2004. Neoproterozoic—Early Paleozoic evolution of peri-Gondwanan terranes: Implications for Laurentia-Gondwana connections. Int. J. Earth Sci. 93, 659-682.
Murphy, J. B., Strachan, R. A., Nance, R. D., Parker, K. D., Fowler, M. B., 2000. Proto-Avalonia: a 1.2–1.0 Ga tectonothermal event and constraints for the evolution of Rodinia. Geology 28, 1071-1074.
Nance, R. D., Murphy, J. B., 1994. Contrasting basement isotopic signatures and the palinspastic restoration of peripheral orogens: Example from the Neoproterozoic Avalonian-Cadomian belt. Geology 22, 617-620.
Normore, L. S., 2011. Preliminary findings on the geology of the Trinity map area (NTS 2C/06), Newfoundland, in current Research: Newfoundland and Labrador Department of Natural Resources: Geological Survey Report 11-1, p. 273-293.
Normore, L.S. 2010. Geology of the Bonavista map area (NTS 2C/11), Newfoundland, in Current research. Newfoundland and Labrador Department of Natural Resources: Geological Survey Report 10-1, p. 281–301.
O'Brien, S. J., King, A. F., 2005. Late Neoproterozoic (Ediacaran) stratigraphy of Avalon Zone sedimentary rocks, Bonavista Peninsula, Newfoundland, in Current Research, Newfoundland and Labrador Department of Natural Resources Geological Survey 5, p. 101-113.
O'Brien, S.J., O'Brien, B.H., Dunning, G.R., Tucker, R.D. 1996. Late Neoproterozoic Avalonian and related peri-Gondwanan rocks of the Newfoundland Appalachians. Geol. Soc. Am., Special Paper 304, 9–28.
Pisarevsky, S. A., McCausland, P. J., Hodych, J. P., O'Brien, S. J., Tait, J. A., Murphy, J. B., 2012. Paleomagnetic study of the late Neoproterozoic Bull Arm and Crown Hill formations (Musgravetown Group) of eastern Newfoundland: Implications for Avalonia and West Gondwana paleogeography. Can. J. Earth Sci. 49, 308-327.
Pisarevsky, S. A., Murphy, J. B., Cawood, P.A., Collins, A.S., 2008. Late Neoproterozoic and Early Cambrian palaeogeography: models and problems. Geol. Soc. Spec. Publ. 294, 9-31.

Pollock, J. C., Hibbard, J. P., Sylvester, P. J., 2009. Early Ordovician rifting of Avalonia and birth of the Rheic Ocean: U–Pb detrital zircon constraints from Newfoundland. J. Geol. Soc. 166, 501-515.

Pollock, J. C., Hibbard, J. P., van Staal, C. R., 2012. A paleogeographical review of the peri-Gondwanan realm of the Appalachian orogen. Can. J. Earth Sci. 49, 259-288.

Pu, J. P., Bowring, S. A., Ramezani, J., Myrow, P., Raub, T. D., Landing, E., Mills, A., Hodgin, E., Macdonald, F. A., 2016. Dodging snowballs: Geochronology of the Gaskiers glaciation and the first appearance of the Ediacaran biota. Geology 44, 955-958.

Robert, B., Besse, J., Blein, O., Greff-Lefftz, M., Baudin, T., Lopes, F., Meslouh, S., Belbadaoui, M., 2017. Constraints on the Ediacaran inertial interchange true polar wander hypothesis: A new paleomagnetic study in Morocco (West African Craton). Precambrian Res. 295, 90-116.

Robert, B., Greff-Lefftz, M., Besse, J., 2018. True Polar Wander: A Key Indicator for Plate Configuration and Mantle Convection During the Late Neoproterozoic. Geochem. Geophy. Geosy. 19, 3478-3495.

Schmitt, R.S., Fragoso, R.A., Collins, A.S., 2018. Suturing Gondwana in the Cambrian: The orogenic events of the final amalgamation. In: Geology of Southwest Gondwana–Regional Geology Reviews. 1ed. Springer International Publishing, 63-85.

Sparkes, G.W., Dunning, G.R., 2014. Late Neoproterozoic epithermal alteration and mineralization in the western Avalon zone: a summary of mineralogical investigations and new U/Pb geochronological results, in Current Research: Newfoundland and Labrador Department of Natural Resources: Geological Survey Report 14, p. 99-128.

Steinberger, B., Torsvik, T. H., 2008. Absolute plate motions and true polar wander in the absence of hotspot tracks. Nature 452, 620-623.

Tauxe, L., Shaar, R., Jonestrask, L., Swanson-Hysell, N. L., Minnett, R., Koppers, A. A. P., Constable, C.G., Jarboe, N., Gaastra, K., Fairchild, L., 2016. PmagPy: Software package for paleomagnetic data analysis and a bridge to the Magnetics Information Consortium (MagIC) Database. Geochem. Geophy. Geosy. 17, 2450-2463.

Thompson, M. D., Barr, S. M., Grunow, A. M., 2012. Avalonian perspectives on Neoproterozoic paleogeography: Evidence from Sm-Nd isotope geochemistry and detrital zircon geochronology in SE New England, USA. Geol. Soc. Am. Bull. 124, 517-531.

Thompson, M. D., Grunow, A. M., Ramezani, J., 2007. Late Neoproterozoic paleogeography of the southeastern New England Avalon zone: Insights from U-Pb geochronology and paleomagnetism. Geol. Soc. Am. Bull. 119, 681-696.

Thompson, M. D., Ramezani, J., Crowley, J. L., 2014. U-Pb zircon geochronology of Roxbury Conglomerate, Boston Basin, Massachusetts: Tectono-stratigraphic implications for Avalonia in and beyond SE New England. Am. J. Sci. 314, 1009-1040.

Tohver, E., Cawood, P. A., Rossello, E. A., Jourdan, F., 2012. Closure of the Clymene Ocean and formation of West Gondwana in the Cambrian: Evidence from the Sierras Australes of the southernmost Rio de la Plata craton, Argentina. Gondwana Res. 21, 394-405.

Tohver, E., Trindade, R. I. F. D., Solum, J. G., Hall, C. M., Riccomini, C., Nogueira, A. C., 2010. Closing the Clymene ocean and bending a Brasiliano belt: Evidence for the Cambrian formation of Gondwana, southeast Amazon craton. Geology 38, 267-270.

Torsvik, T. H., Van der Voo, R., Preeden, U., Mac Niocaill, C., Steinberger, B., Doubrovine, P. V., van Hinsbergen, D.J.J., Domeier, M., Gaina, C., Tohver, E., Meert, J.G., McCausland, P.J.A., Cocks, L.R., 2012. Phanerozoic polar wander, palaeogeography and dynamics. Earth Sci. Rev. 114, 325-368.

Trindade, R. I., D'Agrella-Filho, M. S., Epof, I., Neves, B. B. B., 2006. Paleomagnetism of Early Cambrian Itabaiana mafic dikes (NE Brazil) and the final assembly of Gondwana. Earth Planet. Sci. Lett. 244, 361-377.

Van der Voo, R., 1990. The reliability of paleomagnetic data. Tectonophysics 184, 1–9.

van Staal, C. R., Barr, S. M., McCausland, P. J. A., Thompson, M. D., White, C. E., 2020. Tonian-Ediacaran tectonomagmatic evolution of West Avalonia and its Ediacaran-Early Cambrian interactions with Ganderia: An example of complex terrane transfer due to arc-arc collision?. Geol. Soc. Spec. Publ. 503, https://doi.org/10.1144/SP503-2020-23.

Vizan, H., Carney, J. N., Turner, P., Ixer, R. A., Tomasso, M., Mullen, R. P., Clarke, P., 2003. Late Neoproterozoic to Early Palaeozoic palaeogeography of Avalonia: some palaeomagnetic constraints from Nuneaton, central England. Geol. Mag. 140, 685–705.

Waldron, J. W., Schofield, D. I., Pearson, G., Sarkar, C., Luo, Y., Dokken, R., 2019. Detrital zircon characterization of early Cambrian sandstones from East Avalonia and SE Ireland: Implications for terrane affinities in the peri-Gondwanan Caledonides. Geol. Mag. 156, 1217-1232.

Wu, F., Van der Voo, R., Johnson, R. J., 1986. Eocambrian paleomagnetism of the Boston Basin: Evidence for displaced terrane. Geophys. Res. Lett. 13, 1450-1453.

Figure captions

Fig. 1. (A) Location of Avalonia (peri-Gondwana) terranes in a Pangea fit (after Pollock et al., 2009; Henderson et al., 2016; Waldron et al., 2019). (B) Outline of West Avalonia in Newfoundland (inset) and geological map of the study area (modified from O'Brien and King, 2005; Normore, 2010, 2011), showing sampling localities (see detailed stratigraphy and sampling in Fig. 2). Open stars represent the sampling sites in Pisarevsky et al. (2012). (C) Strata of the Musgravetown Group in the study area (after Normore, 2010, 2011) and available age constraints (data are from Pollock et al., 2009; Mills et al., 2016, 2017; Pu et al., 2016). DHBF-Dover-Hermitage Bay Faults.

Fig. 2. Stratigraphic sampling of the Musgravetown Group (Bonavista Basin) in this study, showing the available U-Pb zircon ages (①, Mills et al., 2016; ②, Pu et al., 2016; ③, Pollock et al., 2009).

Fig. 3. Progressive demagnetization behaviors for representative specimens from the Bull Arm (A and B), Big Head (C), Rocky Harbour (D) and Crown Hill (E and F) formations. NRM, natural remanent magnetization; LN2, liquid nitrogen cooling step; T100, demagnetization at 100°C, etc. All projections are in tilt-corrected coordinates.

Fig. 4. Paleomagnetic results of the Bull Arm (blue; together with data from Pisarevsky et al., 2012) and Crown Hill formations (pink). (A–B) Equal-area stereographic projections for the directions in *in-situ* and tilt-corrected coordinates, respectively. Solid/open symbols represent the lower/upper hemisphere projections. (C–D) Parametric bootstrap fold tests (Tauxe et al., 2016) for the ChRMs of Bull Arm and Crown Hill formations. T_1/CDF, maximum eigenvalue/cumulative distribution function (CDF) of the percent unfolding.

Fig. 5. Distribution of ChRMs from the red sandstone pebbles of Rocky Harbour Formation, showing an inconclusive conglomerate test. b1 and b2 are drilled from the same clast. Solid/open squares represent the lower/upper hemisphere directions.

Fig. 6. Directions of the low temperature components (LTCs) for samples from the Crown Hill Formation. Dg/Ds, Ig/Is, and Kg/Ks, declination, inclination and precision parameter for the directions in geographic (A) and stratigraphic (B) coordinates, respectively. Mean directions are shown with stars and α95 confidence ovals. PEF, present Earth's field.

Fig. 7. (A) Apparent polar wander path (APWP) of Avalonia terrane, showing the large polar motion from ca. 590-575 to 560 Ma. See pole list and abbreviations in Table 2. Avalonia composite terrane is restored by rotating East Avalonia (79.1°N, -163.0°E, -34.8°) and New England (43.1°N, -73.6°E, 92.8°) to Newfoundland. The dispersion of Newfoundland poles can be explained by modest amounts of local vertical-axis rotations between the sampled regions, and/or minor APW within the 600-575 Ma interval. (B) Fitting the mid–late Ediacaran APWP segment of Avalonia with the coeval paleomagnetic poles (Table S1) from West Africa and Laurentia after Robert et al. (2017), showing the four possible positions of Avalonia (Euler pole for preferred position #1, Newfoundland to West Africa: 5.8°S, 158.8°E, -84.1°). Dashed-line and unshaded version for pole CH includes correction for a plausible amount of inclination shallowing (f=0.6).

Fig. 8. (A) The mid-late Ediacaran APWP fits (in West African coordinates) and (B) reconstruction of West Gondwana at ca. 590-575 Ma in an absolute reference frame with a Baltica-Avalonia juxtaposition, showing the oft-suggested but paleomagnetically invalid 'X' position of Avalonia (poles shown in gray color; Euler rotation: 41.9°N, 12.3°E, 54.5°). Baltica is rotated to West Africa using Euler rotation (0.2°N, -169.0°E, -117.9°). The poles from Laurentia are rotated to West Africa after Robert et al. (2017). Pole list and abbreviations are in Tables 2 and S1. (C and D) As in (A) and (B), but with Amazonia (12.9°S, 36.7°E, 327.1°) juxtaposed to Avalonia and showing the optimal match for Baltica (see the main text; Euler rotation: 8.4°N, 3.5°E, 92.7°). SF = São Francisco; RP = Río de La Plata; PR = Parnaíba (after Schmitt et al., 2018); AAT = Arequipa-Antofalla Terrane (after Escayola et al., 2011).

Table captions

Table 1. Summary of paleomagnetic results in this study. S-lat/S-long, latitude and longitude for sampling sites; n/n0, number of specimens for mean direction calculation/number of specimens demagnetized; Dg/Ig and Ds/Is, declination and inclination in geographic and stratigraphic coordinates, respectively; A95/α95, radius of 95% confidence circle; MAD, maximum angular deviation; k, precision parameter; PEF, present Earth's field. *Excluded from final calculation; Sites with "a" are from Pisarevsky et al., 2012.

Table 2. Ediacaran paleomagnetic poles of Avalonia composite terrane. Notes: P-lat/P-long, latitude/longitude of paleomagnetic pole. A95, the radius of the paleomagnetic pole 95% confidence limits. Q_f, Q-factor of Van der Voo, 1990. "*" represents poles not used in Fig. 7.

Figure

Click here to download Figure: Fig 1-Tectonic framework and localities.pdf

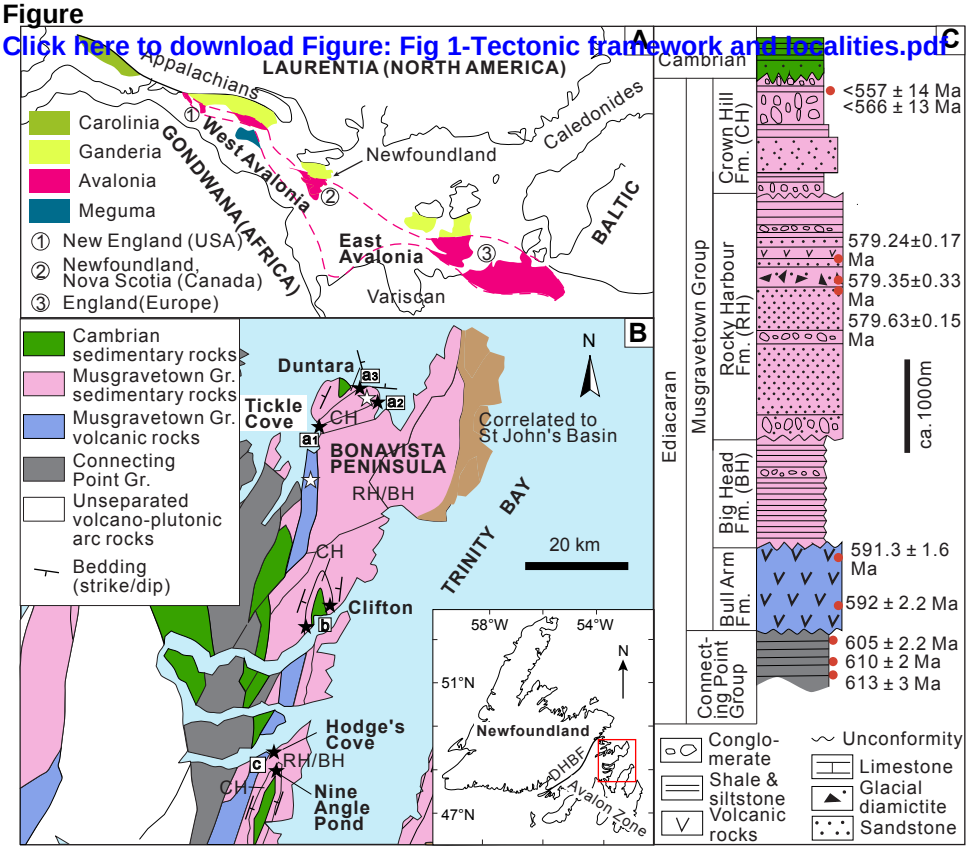

Figure

Click here to download Figure: Fig.2-strata and sites.pdf

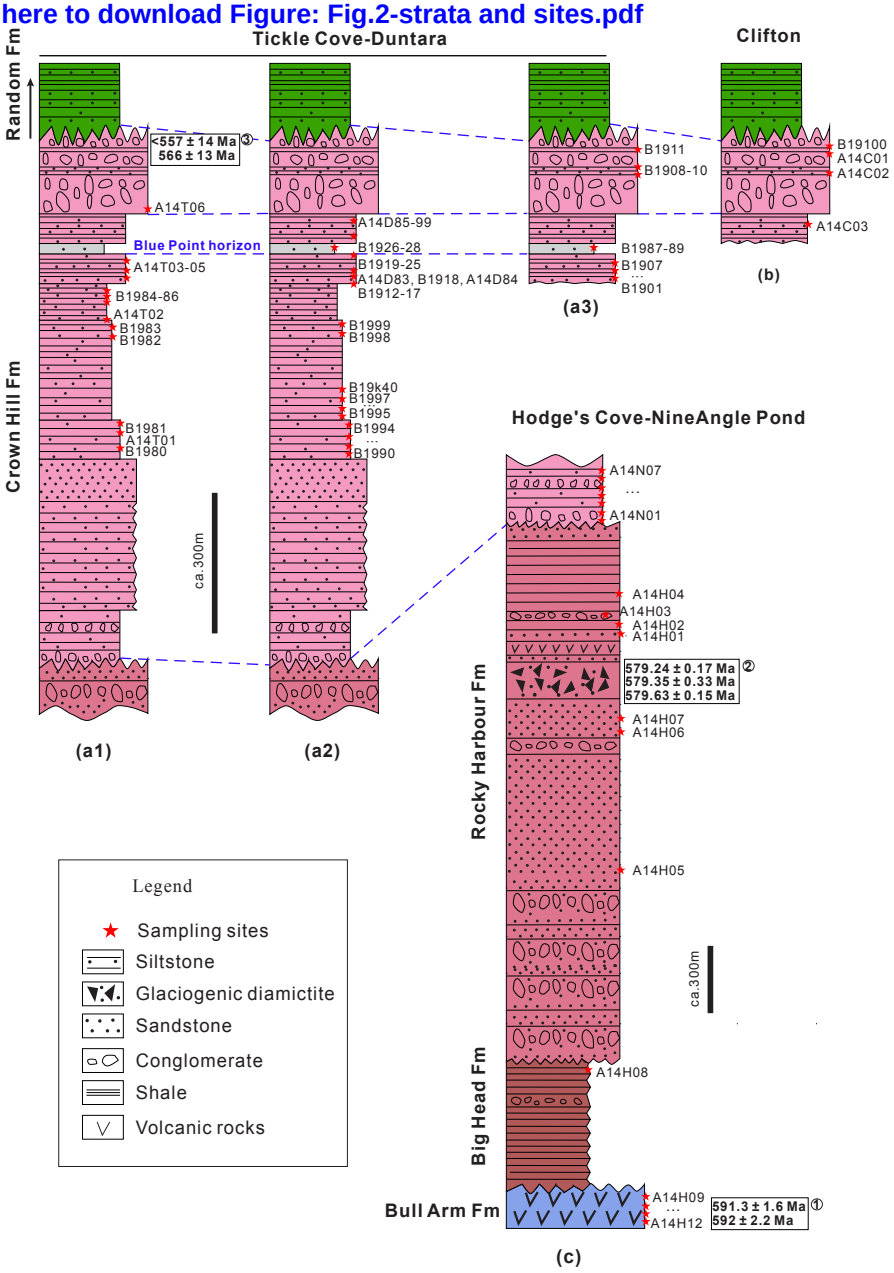

Figure

Click here to download Figure: Fig.3-Demagnetizations.pdf

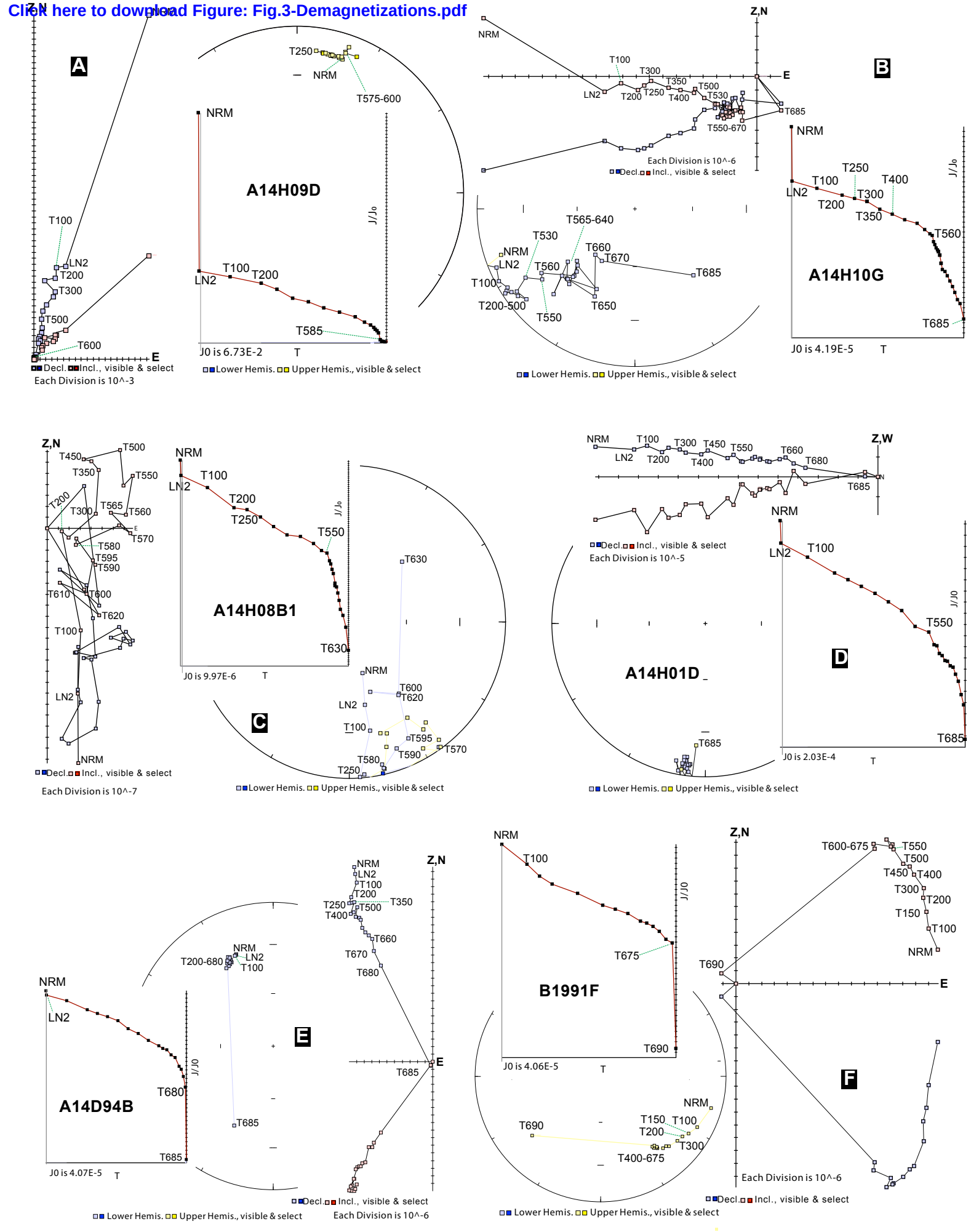

Figure

Click here to download Figure: Fig.4-Paleomagnetic results and test.pdf

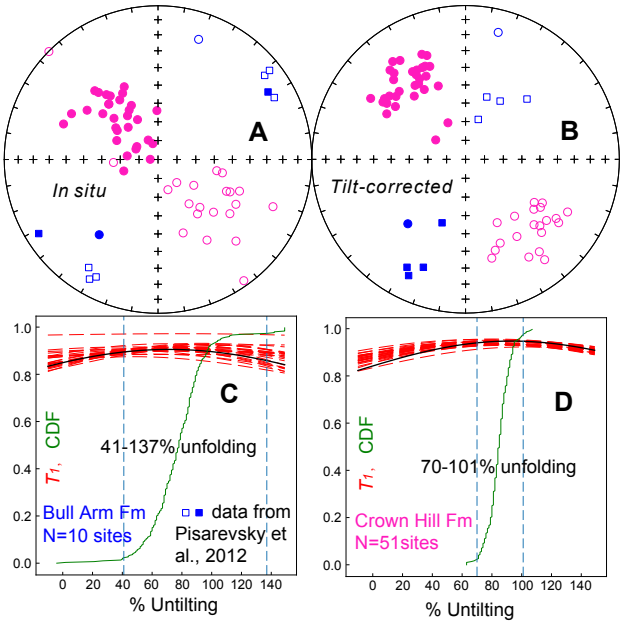

Figure

Click here to download Figure: Fig.5-Conglomerate test.pdf

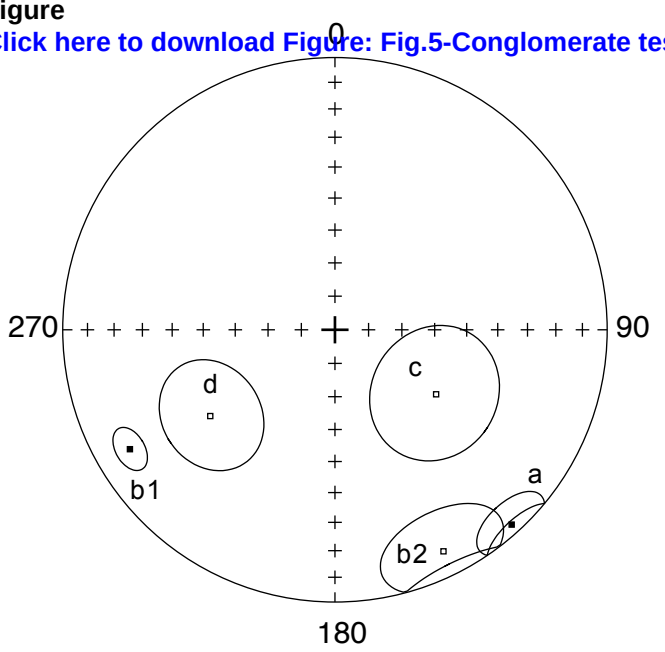

Figure

Click here to download Figure: Fig.6-LTCs of CH.pdf

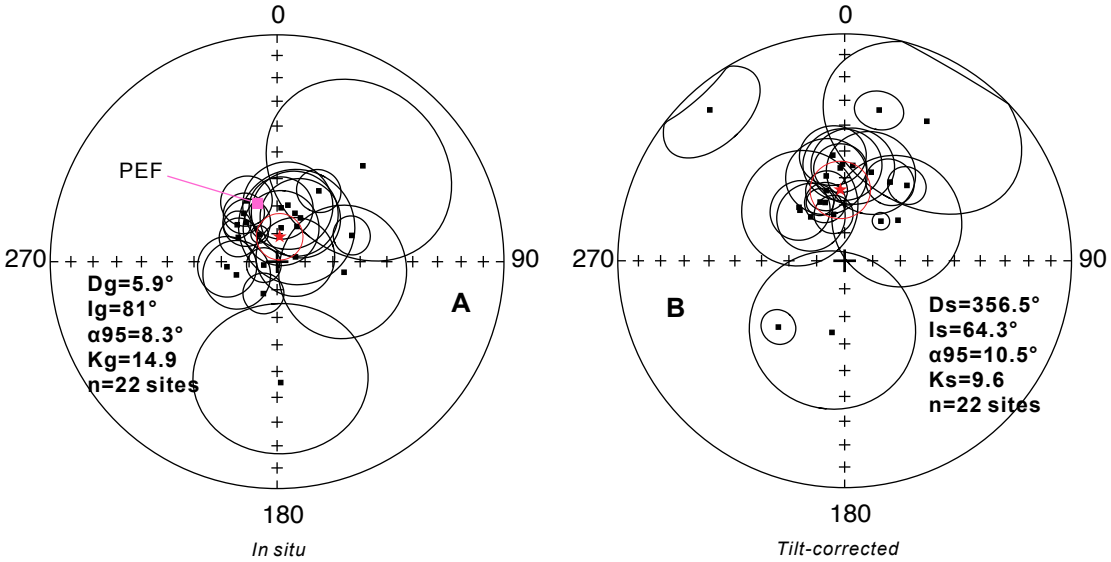

Figure

Click here to download Figure: Fig.7-Avalonia_APWP.pdf

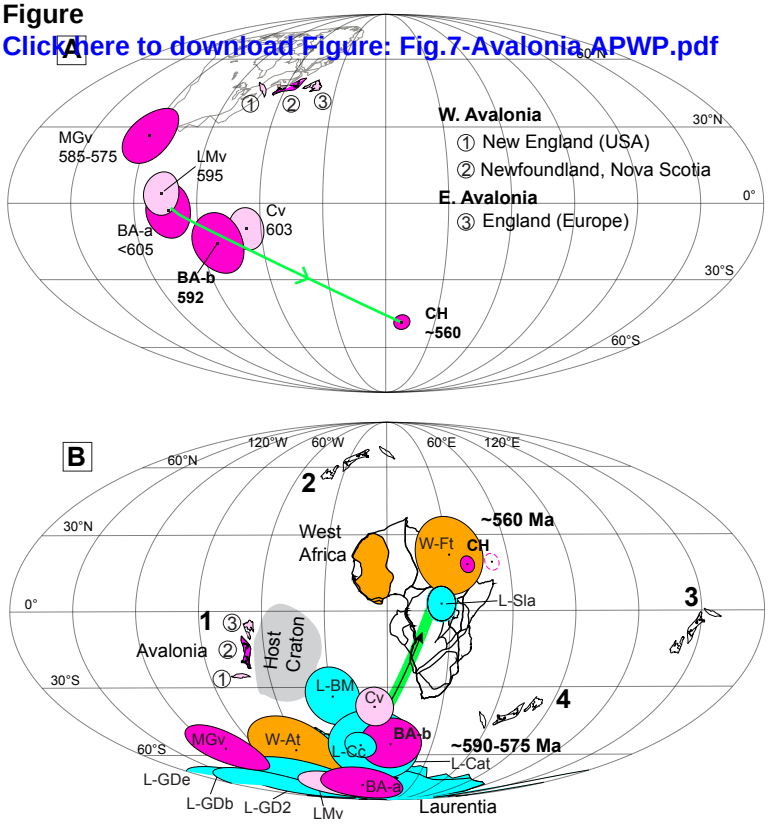

Figure

Click here to download Figure: Fig.8-Reconstruction.pdf

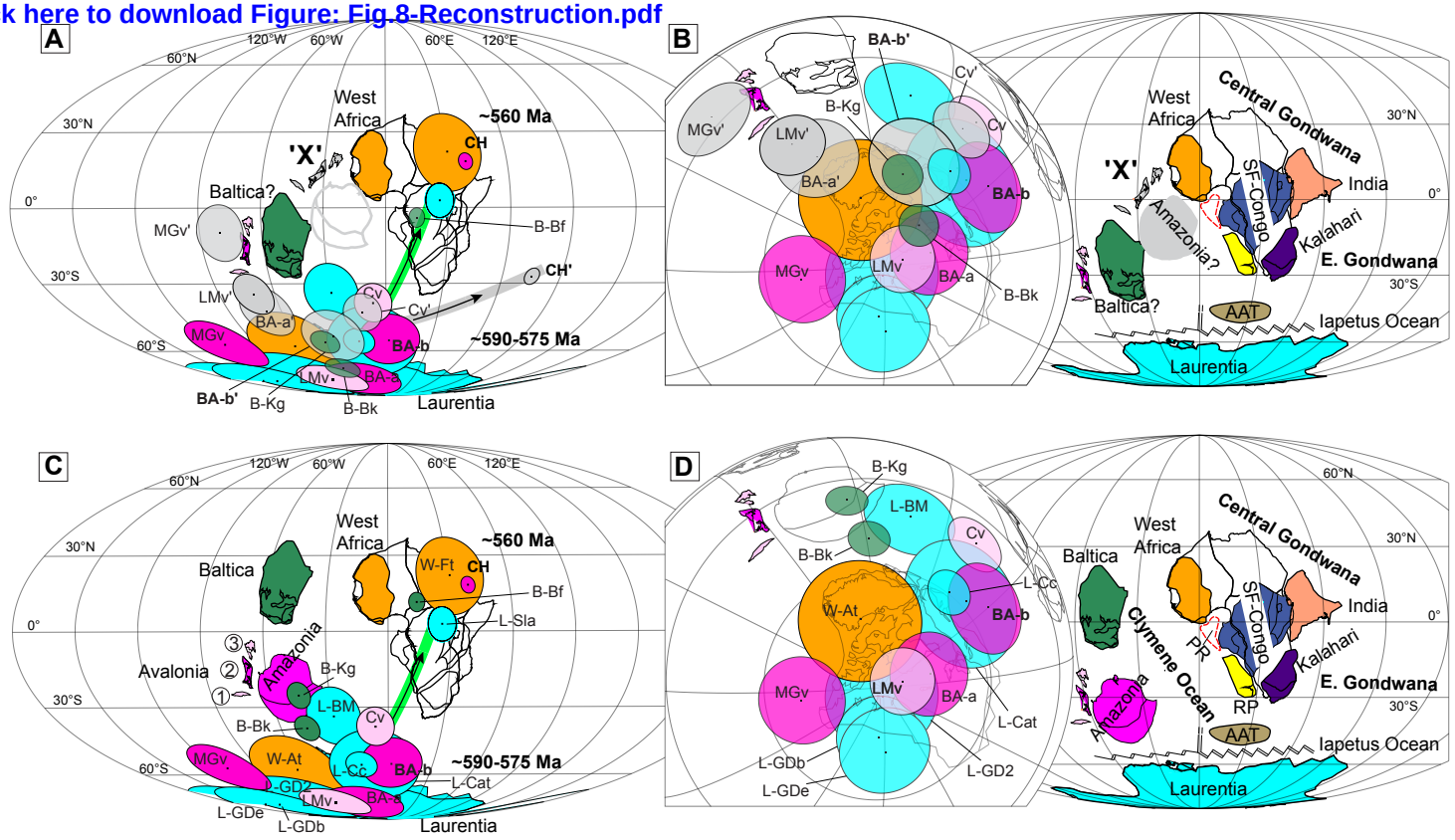

Table

Click here to download Table: Table 1-Summary of paleomagnetic data.xlsx

Table 1 Summary of paleomagnetic results in this study

Section	Site	Stratigraphic Unit	S-Lat	S-Long	Strike	Dip	n/n_0	D_g
Clifton	B19100	Crown Hill Fm	48°10'30.70"N	53°38'55.10"W	208	71	6/17	266.2
	A14C01	Crown Hill Fm	48°10'39.58"N	53°39'55.08"W	86	24	4/7	144.7
	A14C02*	Crown Hill Fm	48°10'39.54"N	53°39'56.05"W	61	33	5/8	122.1
	A14C03*	Crown Hill Fm	48°10'46.92"N	53°40'19.78"W	46	36	9/9	335.2
Tickle Cove-Duntara	B1911	Crown Hill Fm	48°36'16.40"N	53°23'45.40"W	130	30	9/10	148.7
	B1910	Crown Hill Fm	48°36'16.60"N	53°23'36.30"W	195	25	2/8	333.8
	B1909*	Crown Hill Fm	48°36'16.60"N	53°23'36.30"W	195	25	5/6	359.4
	B1908*	Crown Hill Fm	48°36'16.60"N	53°23'36.30"W	230	40	0/8	—
	A14T06*	Crown Hill Fm	48°35'21.48"N	53°28'49.80"W	46	15	0/8	—
	A14D99	Crown Hill Fm	48°35'50.96"N	53°21'19.22"W	275	27	3/3	145.0
	A14D98	Crown Hill Fm	48°35'50.57"N	53°21'19.98"W	275	27	4/4	327.3
	A14D97*	Crown Hill Fm	48°35'51.07"N	53°21'20.30"W	283	16	3/3	288.3
	A14D96	Crown Hill Fm	48°35'51.11"N	53°21'20.92"W	283	16	3/3	318.3
	A14D95	Crown Hill Fm	48°35'51.36"N	53°21'22.57"W	283	16	3/3	136.3
	A14D94	Crown Hill Fm	48°35'50.06"N	53°21'26.39"W	274	16	3/3	323.1
	A14D93	Crown Hill Fm	48°35'49.74"N	53°21'26.60"W	274	16	2/3	331.9
	A14D92	Crown Hill Fm	48°35'49.85"N	53°21'26.93"W	284	18	3/3	309.7
	A14D91	Crown Hill Fm	48°35'49.38"N	53°21'28.73"W	284	18	3/3	144.0
	A14D90*	Crown Hill Fm	48°35'49.56"N	53°21'29.23"W	286	14	3/3	332.0
	A14D89	Crown Hill Fm	48°35'48.80"N	53°21'32.54"W	294	19	3/3	321.5
	A14D88	Crown Hill Fm	48°35'49.16"N	53°21'35.96"W	266	13	4/4	127.0
	A14D87	Crown Hill Fm	48°35'49.78"N	53°21'42.77"W	285	16	2/3	133.5
	A14D86*	Crown Hill Fm	48°35'49.96"N	53°21'42.84"W	285	16	0/3	—
	A14D85	Crown Hill Fm	48°35'48.66"N	53°21'45.22"W	285	16	3/3	119.9
	B1987	Crown Hill Fm	48°36'20.21"N	53°21'58.33"W	253	21	8/8	318.4
	B1988	Crown Hill Fm	48°36'18.99"N	53°21'59.06"W	250	26	6/6	317.2
	B1989*	Crown Hill Fm	48°36'16.81"N	53°22'0.02"W	250	26	5/7	139.1
	B1928*	Crown Hill Fm	48°35'48.90"N	53°21'45.50"W	249	20	0/3	—
	B1927*	Crown Hill Fm	48°35'48.30"N	53°21'46.80"W	250	20	0/4	—
	B1926*	Crown Hill Fm	48°35'48.30"N	53°21'46.80"W	250	20	3/3	3.7
	B1925*	Crown Hill Fm	48°35'48.30"N	53°21'46.80"W	252	20	5/5	129.3
	B1907	Crown Hill Fm	48°36'10.10"N	53°21'57.10"W	322	13	6/10	112.3
	B1924	Crown Hill Fm	48°35'48.30"N	53°21'46.80"W	252	20	3/3	101.7
	B1923	Crown Hill Fm	48°35'48.30"N	53°21'46.80"W	253	20	4/4	114.9
	B1922	Crown Hill Fm	48°35'48.30"N	53°21'46.80"W	256	20	2/4	100.8
	B1921	Crown Hill Fm	48°35'48.30"N	53°21'46.80"W	255	20	4/4	335.1
	B1920	Crown Hill Fm	48°35'48.30"N	53°21'46.80"W	254	20	4/4	329.7
	B1919	Crown Hill Fm	48°35'48.30"N	53°21'46.80"W	255	20	4/4	271.4
	A14D84*	Crown Hill Fm	48°35'48.16"N	53°21'52.70"W	278	13	0/3	—
	B1918	Crown Hill Fm	48°35'49.20"N	53°21'53.90"W	279	17	4/4	325.1
	A14D83	Crown Hill Fm	48°35'48.73"N	53°21'53.86"W	275	18	3/3	318.5
	B1917	Crown Hill Fm	48°35'48.90"N	53°21'52.70"W	279	17	4/4	313.1

Table

Click here to download Table: Table 2-Paleopoles compilation from Avalonia .xlsx

Pole ID	Rock Unit (Area)	Age (Ma)	Age range Max
West Avalonia			
CH	**Crown Hill Fm, Newfoundland, Canada**	**< 557+/-14 Ma; 566+/-13**	**570**
BA-b	**Bonavista Bull Arm Fm, Newfoundland, Canada**	**592 ± 2.2; 591.3 ± 1.6**	**594**
BA-a	Argentia Bull Arm Formation, Newfoundland, Canada	< 605	
MGv	Marystown Group volcanic-sedimentary sequence, Newfoundland, Canada	585 ± 2; 580 ± 3; 576.8 ± 2.6; 575 ± 2	587
Rf*	Roxbury Formation, New England, USA	~ 582 Ma, correlation to Gaskiers (Pu et al., 2016)	593
LMv	Lynn-Mattapan Volcanics, New Englend, USA	595.8 ± 1.2; 597.4 ± 1.5; 596.0 ± 1.4; 595.7 ± 1.6	599
East Avalonia			
Cv	Caldecote Volcanics, England	603 ± 2	605